C. R. Mecanique 339 (2011) 674–681

Contents lists available at ScienceDirect

Comptes Rendus Mecanique

www.sciencedirect.com

Identification of internal cracks in a three-dimensional solid body via Steklov–Poincaré approaches

Identification de fissures dans un solide tridimentionnel au moyen d'approches du type Steklov–Poincaré

Mohamed Larbi Kadri [a], Jalel Ben Abdallah [a,*], Thouraya Nouri Baranger [b]

[a] *Université El Manar, LAMSIN, École nationale d'ingénieurs de Tunis, BP no. 37, 1002 Tunis, Tunisia*
[b] *Université de Lyon, CNRS, université Lyon 1, LaMCoS UMR 5259, INSA-Lyon, 18-20, rue des sciences, 69621 Villeurbanne cedex, France*

ARTICLE INFO

Article history:
Received 25 November 2010
Accepted after revision 24 June 2011
Available online 30 July 2011

Keywords:
Computational solid mechanics
Crack identification
Data completion
Inverse problem
Cauchy problem
Steklov–Poincaré equations

Mots-clés :
Mécanique des solides numérique
Identification de fissures
Complétion de données
Problème inverse
Problème de Cauchy
Équations de Steklov–Poincaré

ABSTRACT

This Note deals with the identification of internal planar cracks inside a three-dimensional elastic body via two approaches relying on domain decomposition using elastostatic measurements. These approaches consist in recasting the problem in terms of primal or dual Steklov–Poincaré equations. The primal approach is a straightforward continuation to the elastic Cauchy problem of the work presented in J. Ben Abdallah (2007) [1] which is devoted to the Cauchy problem for the scalar Laplace equation. The numerical performances of these formulations are compared.

RÉSUMÉ

Cette Note concerne la résolution numérique du problème d'identification de fissures planes dans un solide élastique tridimentionnel, via deux approches issues de la décomposition de domaine, à l'aide de mesures élastostatiques. Ces approches consistent à reformuler le problème en termes d'équations de Steklov–Poincaré primale et duale. L'approche primale a fait l'objet d'une étude numérique dans le cadre de l'équation de Laplace J. Ben Abdallah (2007) [1]. Les performances numériques des deux approches sont comparées entre elles.

Version française abrégée

On s'interesse dans cette note au problème inverse d'identification de fissures planes dans un solide élastique tridimentionnel à l'aide de mesures élastostatiques. Le plan dans lequel se situent les fissures doit être connu *a priori* (typiquement un défaut de délaminage). La reconstruction des fissures est ramenée à la résolution de deux problèmes de complétion de données à l'aide de mesures élastostatiques. Chacun de ces deux problèmes aux dérivées partielles est connu sous le nom de problème de Cauchy : on considère un solide élastique occupant un domaine Ω, de frontière Γ de normale unitaire $\mathbf{n}$. Soit (Γ_i, Γ_c) une partition de Γ. Si $\mathcal{A}$ désigne le tenseur de Hooke du matériau constitutif du solide, le problème de Cauchy

* Corresponding author.
E-mail addresses: medlarbi.kadri@lamsin.rnu.tn (M.L. Kadri), jalel.benabdallah@enit.rnu.tn (J. Ben Abdallah), Thouraya.baranger@univ-lyon1.fr (T.N. Baranger).

1631-0721/$ – see front matter
doi:10.1016/j.crme.2011.06.004

est donné par le système d'équations au dérivées partielles (1) ayant pour données l'effort imposé $\tilde{\boldsymbol{t}}$ et les déplacements mesurés $\tilde{\boldsymbol{u}}$ sur Γ_c. Cependant sur la frontière Γ_i aucune donnée n'est disponible. La résolution du problème de Cauchy permet d'identifier les données manquantes, à savoir le couple $(\boldsymbol{u}_i, \boldsymbol{t}_i)$ des déplacements et des efforts sur Γ_i. Ce problème est connu pour être mal posé au sens de Hadamard [2]. On se propose ici de le résoudre à l'aide d'outils issus de la décompostion de domaine [3] : l'équation de Steklov–Poincaré (6) et l'équation de Steklov–Poincaré duale (8). Chacune d'elles consiste à reformuler le problème et aboutit à une équation régie par un opérateur de bord. L'approche primale a été introduite et analysé dans [4–6] pour la résolution du problème de Cauchy–Poisson. Une étude numérique de cette approche a été réalisée dans le cadre de l'opérateur de Laplace dans [1]. Un cadre général regroupant les différentes approches, primale, duale et mixte est présenté dans [7].

Les deux méthodes sont mise en œuvre numériquement et leurs performances comparées à travers un exemple d'identification de fissures dans un domaine élastique tridimensionnel. Ces deux approches sont également comparées à la méthode de Kozlov–Maz'ya–Fomin (KMF) [8]. Pour l'identification des fissures, deux problèmes de Cauchy sont résolus afin de reconstruire le champ de déplacement sur l'interface fissurée. La discontinuité des déplacements reconstruits à travers cette interface constitue le support des fissures recherchées. Les résultats montrent que l'approche duale est plus performante que l'approche primale, elle même plus efficace que la méthode KMF. La supériorité de l'approche duale n'est pas intrinsèque à celle-ci mais dépend fortement de l'application (singularité des données de Cauchy, de la géométrie, etc.) comme le suggère la référence [7]. Cependant, cette comparaison ne tient pas compte de la possibilité d'utiliser des préconditionneurs avec l'une où l'autre des approches. Cet aspect fait l'objet d'une étude en cours.

1. Introduction

In this work we consider the problem of cracks identification in a three-dimensional elastic body by using overspecified elastostatic data measured on the external boundary of the domain. The cracks are supposed to be lying in *a priori* known planar interface, this kind of problem arises in non-destructive inspection of materials, such as coating defect or delamination identification in a composite material. Two data completion problems are then solved on the two subdomains separated by the cracks carrying interface. The mathematical formulation corresponding to data completion problem is the well-known Cauchy problem which can be written as follows.

A linear elastic material occupies an open bounded domain Ω with smooth boundary Γ where $\mathbf{n}$ is the outward normal vector. We denote the boundary where the overspecified data can be measured and the boundary where the data have to be recovered by Γ_c and Γ_i respectively. The Cauchy problem can be stated as follows: find $(\boldsymbol{u}_i, \boldsymbol{t}_i)$ on Γ_i such that a displacement field $\boldsymbol{u}$ exists that satisfies:

$$\begin{cases} -\operatorname{div}\boldsymbol{\sigma}\big(\boldsymbol{u}(x)\big) = \boldsymbol{f}(x) & \text{in } \Omega \\ \boldsymbol{u}(x) = \tilde{\boldsymbol{u}}(x) & \text{on } \Gamma_c \\ \boldsymbol{\sigma}\big(\boldsymbol{u}(x)\big)\mathbf{n}(x) = \tilde{\boldsymbol{t}}(x) & \text{on } \Gamma_c \end{cases} \tag{1}$$

where $\boldsymbol{\sigma}$ is the stress tensor and $\boldsymbol{f}$ is the volume force. $\tilde{\boldsymbol{u}}$ and $\tilde{\boldsymbol{t}}$ are the given displacement and traction vectors respectively. Fields $\boldsymbol{\sigma}$ and $\boldsymbol{u}$ are related by the linear elastic constitutive law $\boldsymbol{\sigma}(\boldsymbol{u}) = \boldsymbol{\mathcal{A}} : \nabla \boldsymbol{u}$, where $\boldsymbol{\mathcal{A}}$ is Hooke's tensor. This problem is known to be ill-posed in the sense that the solution does not depend continuously on the data [2]. In the literature, several authors have studied the Cauchy problem in linear elasticity by using different approaches. In [9] the authors proposed an alternative formulation of the regularization based on the indirect fictitious boundary method; the optimization of an energy-like functional is used in [10–12] and applied to two-dimensional and three-dimensional contact and interfacial identification problems; and in [13], the authors used an alternating direction iterative method to solve Cauchy problem in order to identify interlaminar cracks.

In this paper we propose to recover the data lacking on Γ_i by using the primal and dual Steklov–Poincaré equations which are commonly used in domain decomposition [3]. The primal approach was introduced for the Cauchy problem of the Laplace equation in [4,5]. The paper [1] was devoted to the numerical study of the primal approach for the Laplace equation by using a conjugate gradient type method.

A general framework for the different approaches (primal, dual and mixed) is presented in [7]. In this paper, the dual and primal approaches are used in order to solve the above Cauchy problem.

In Section 2 we recast the problem (1) in condensed form which leads to the Cauchy–Steklov–Poincaré equation acting on the boundary of the unknowns. The dual form of the equation introduced is presented in Section 3. Both methods are implemented numerically to identify cracks in a three-dimensional elastic body. The results are presented in Section 4 and the conclusions are given in the last section.

2. The Cauchy–Steklov–Poincaré equation

Let $\boldsymbol{\lambda}$ denote the unknown displacement vector on Γ_i. We consider both Dirichlet and Neumann elliptic problems obtained by duplicating the solution $\boldsymbol{u}$ in a couple of vectors $(\boldsymbol{u}_D, \boldsymbol{u}_N)$. The Cauchy problem (1) is then split into:

$$\begin{cases} -\operatorname{div}\boldsymbol{\sigma}(\boldsymbol{u}_D) = \boldsymbol{f} & \text{in } \Omega \\ \boldsymbol{u}_D = \tilde{\boldsymbol{u}} & \text{on } \Gamma_c \\ \boldsymbol{u}_D = \boldsymbol{\lambda} & \text{on } \Gamma_i \end{cases} \quad \text{and} \quad \begin{cases} -\operatorname{div}\boldsymbol{\sigma}(\boldsymbol{u}_N) = \boldsymbol{f} & \text{in } \Omega \\ \boldsymbol{\sigma}(\boldsymbol{u}_N)\mathbf{n} = \tilde{\boldsymbol{t}} & \text{on } \Gamma_c \\ \boldsymbol{u}_N = \boldsymbol{\lambda} & \text{on } \Gamma_i \end{cases}$$

If the pair $(\tilde{\boldsymbol{u}}, \tilde{\boldsymbol{t}})$ is compatible (i.e. a vector field $\boldsymbol{u}$ exists that verifies the equation $-\operatorname{div}\boldsymbol{\sigma}(\boldsymbol{u}) = \boldsymbol{f}$ in Ω for which $(\tilde{\boldsymbol{u}}, \tilde{\boldsymbol{t}})$ are the Cauchy data on Γ_c), the solution of the Cauchy problem is recovered, i.e. $\boldsymbol{u} = \boldsymbol{u}_D = \boldsymbol{u}_N$ in Ω, if and only if:

$$\boldsymbol{\sigma}\big(\boldsymbol{u}_D(\boldsymbol{\lambda})\big)\mathbf{n} = \boldsymbol{\sigma}\big(\boldsymbol{u}_N(\boldsymbol{\lambda})\big)\mathbf{n} \quad \text{on } \Gamma_i \tag{2}$$

Now for $\boldsymbol{\mu}$, a displacement field defined on Γ_i, the linear parts of $\boldsymbol{u}_N(\boldsymbol{\mu})$ and $\boldsymbol{u}_D(\boldsymbol{\mu})$ are denoted $\boldsymbol{u}_N^0(\boldsymbol{\mu})$ and $\boldsymbol{u}_D^0(\boldsymbol{\mu})$ which solve respectively:

$$\begin{cases} -\operatorname{div}\boldsymbol{\sigma}\big(\boldsymbol{u}_D^0(\boldsymbol{\mu})\big) = \mathbf{0} & \text{in } \Omega \\ \boldsymbol{u}_D^0(\boldsymbol{\mu}) = 0 & \text{on } \Gamma_c \\ \boldsymbol{u}_D^0(\boldsymbol{\mu}) = \boldsymbol{\mu} & \text{on } \Gamma_i \end{cases} \quad \text{and} \quad \begin{cases} -\operatorname{div}\boldsymbol{\sigma}\big(\boldsymbol{u}_N^0(\boldsymbol{\mu})\big) = \mathbf{0} & \text{in } \Omega \\ \boldsymbol{t} = \boldsymbol{\sigma}\big(\boldsymbol{u}_N^0(\boldsymbol{\mu})\big)\mathbf{n} = \mathbf{0} & \text{on } \Gamma_c \\ \boldsymbol{u}_N^0(\boldsymbol{\mu}) = \boldsymbol{\mu} & \text{on } \Gamma_i \end{cases} \tag{3}$$

We consider also $\boldsymbol{u}_D^*$ and $\boldsymbol{u}_N^*$ such that:

$$\begin{cases} -\operatorname{div}\boldsymbol{\sigma}\big(\boldsymbol{u}_D^*\big) = \boldsymbol{f} & \text{in } \Omega \\ \boldsymbol{u}_D^* = \tilde{\boldsymbol{u}} & \text{on } \Gamma_c \\ \boldsymbol{u}_D^* = \mathbf{0} & \text{on } \Gamma_i \end{cases} \quad \text{and} \quad \begin{cases} -\operatorname{div}\boldsymbol{\sigma}\big(\boldsymbol{u}_N^*\big) = \boldsymbol{f} & \text{in } \Omega \\ \boldsymbol{t} = \boldsymbol{\sigma}\big(\boldsymbol{u}_N^*\big)\mathbf{n} = \tilde{\boldsymbol{t}} & \text{on } \Gamma_c \\ \boldsymbol{u}_N^* = \mathbf{0} & \text{on } \Gamma_i \end{cases} \tag{4}$$

By superposition, we have $\boldsymbol{u}_D(\boldsymbol{\mu}) = \boldsymbol{u}_D^0(\boldsymbol{\mu}) + \boldsymbol{u}_D^*$ and $\boldsymbol{u}_N(\boldsymbol{\mu}) = \boldsymbol{u}_N^0(\boldsymbol{\mu}) + \boldsymbol{u}_N^*$. With this partition, condition (2) leads to the boundary equation

$$\boldsymbol{\sigma}\big(\boldsymbol{u}_D^0(\boldsymbol{\lambda})\big)\mathbf{n} - \boldsymbol{\sigma}\big(\boldsymbol{u}_N^0(\boldsymbol{\lambda})\big)\mathbf{n} = \boldsymbol{\sigma}\big(\boldsymbol{u}_N^*\big)\mathbf{n} - \boldsymbol{\sigma}\big(\boldsymbol{u}_D^*\big)\mathbf{n} \quad \text{on } \Gamma_i \tag{5}$$

Using the following notations: $\boldsymbol{S}_D(\boldsymbol{\lambda}) = \boldsymbol{\sigma}(\boldsymbol{u}_D^0(\boldsymbol{\lambda}))\mathbf{n}$, $\boldsymbol{S}_N(\boldsymbol{\lambda}) = \boldsymbol{\sigma}(\boldsymbol{u}_N^0(\boldsymbol{\lambda}))\mathbf{n}$, and $\boldsymbol{\chi} = (\boldsymbol{\sigma}(\boldsymbol{u}_N^*) - \boldsymbol{\sigma}(\boldsymbol{u}_D^*))\mathbf{n}$, Eq. (5) becomes:

$$\boldsymbol{S}(\boldsymbol{\lambda}) = \boldsymbol{S}_D(\boldsymbol{\lambda}) - \boldsymbol{S}_N(\boldsymbol{\lambda}) = \boldsymbol{\chi} \quad \text{on } \Gamma_i \tag{6}$$

Eq. (6) is called the Steklov–Poincaré (SP) boundary equation and $\boldsymbol{S}$ is the Steklov–Poincaré operator. It is familiar in the domain decomposition framework for the direct boundary value problem [3]. More precisely, things happen as if vectors $\boldsymbol{u}_D$ and $\boldsymbol{u}_N$ were defined on two different domains with common boundary Γ_i. In this case, Eq. (6) expresses the Neumann transmission condition, but the $(-)$ sign in $\boldsymbol{S}$ would be $(+)$ in the domain decomposition formulation. The $(-)$ sign which appears in $\boldsymbol{S}$ illustrates the ill-posedness of the Cauchy problem [6].

3. The Dual Cauchy–Steklov–Poincaré equation

The Dual Steklov–Poincaré (DSP) problem consists in introducing $\boldsymbol{\lambda} = (\boldsymbol{\sigma}(\boldsymbol{u})\ \mathbf{n})_{|\Gamma_i}$ as the unknown rather than $\boldsymbol{u}_{|\Gamma_i}$. To write the Dual Steklov–Poincaré equation (DSP) on Γ_i we use the same process as that used for the primal formulation. We again consider both Dirichlet and Neumann elliptic problems obtained by duplicating the solution $\boldsymbol{u}$ into a couple of vectors $(\boldsymbol{u}_N, \boldsymbol{u}_D)$. The Cauchy problem (1) is then split into:

$$\begin{cases} -\operatorname{div}\boldsymbol{\sigma}(\boldsymbol{u}_D) = \boldsymbol{f} & \text{in } \Omega \\ \boldsymbol{u}_D = \tilde{\boldsymbol{u}} & \text{on } \Gamma_c \\ \boldsymbol{\sigma}(\boldsymbol{u}_D)\mathbf{n} = \boldsymbol{\lambda} & \text{on } \Gamma_i \end{cases} \quad \text{and} \quad \begin{cases} -\operatorname{div}\boldsymbol{\sigma}(\boldsymbol{u}_N) = \boldsymbol{f} & \text{in } \Omega \\ \boldsymbol{t} = \boldsymbol{\sigma}(\boldsymbol{u}_N)\mathbf{n} = \tilde{\boldsymbol{t}} & \text{on } \Gamma_c \\ \boldsymbol{\sigma}(\boldsymbol{u}_N)\mathbf{n} = \boldsymbol{\lambda} & \text{on } \Gamma_i \end{cases} \tag{7}$$

The DSP equation is obtained by writing $\boldsymbol{u}_D(\boldsymbol{\lambda}) = \boldsymbol{u}_N(\boldsymbol{\lambda})$ on Γ_i which is now the necessary and sufficient condition for solving the Cauchy problem. By splitting $(\boldsymbol{u}_D, \boldsymbol{u}_N)$ into linear parts $(\boldsymbol{u}_D^0, \boldsymbol{u}_N^0)$ and remaining parts $(\boldsymbol{u}_D^*, \boldsymbol{u}_N^*)$, the above relation leads to

$$\boldsymbol{P}(\boldsymbol{\lambda}) = \boldsymbol{P}_D(\boldsymbol{\lambda}) - \boldsymbol{P}_N(\boldsymbol{\lambda}) = \boldsymbol{\psi} \quad \text{on } \Gamma_i \tag{8}$$

with $\boldsymbol{P}_D(\boldsymbol{\lambda}) = \boldsymbol{u}_D^0(\boldsymbol{\lambda})$, $\boldsymbol{P}_N(\boldsymbol{\lambda}) = \boldsymbol{u}_N^0(\boldsymbol{\lambda})$, and $\boldsymbol{\psi} = \boldsymbol{u}_N^* - \boldsymbol{u}_D^*$. We call operator $\boldsymbol{P}$ the Dual Steklov–Poincaré operator, sometimes called the Poincaré–Steklov operator by the domain decomposition community. It is clearly equal to $\boldsymbol{S}_D^{-1} - \boldsymbol{S}_N^{-1}$.

Remark 1. When implementing this approach, it must be kept in mind that the solution of the second PDE system in (7) is defined to within one rigid body motion. In order to overcome this problem, it is possible to devote a well chosen part of Γ_c to set the Dirichlet boundary condition $\tilde{\boldsymbol{u}}$. This approach does not alter the generality of the work presented.

Remark 2. Let us point out that the numerical resolution of the problem (6) is performed without static condensation and that the Schur complement matrix is not explicitly constructed. $\boldsymbol{\chi}$ is calculated once for all by solving Eqs. (4) from which obtain $\boldsymbol{\sigma}(\boldsymbol{u}_N^*)$ and $\boldsymbol{\sigma}(\boldsymbol{u}_D^*)$ on Γ_i. At each iteration k of GMRES the product $\boldsymbol{S}_D\boldsymbol{\lambda}^k$ and $\boldsymbol{S}_N\boldsymbol{\lambda}^k$ are computed by solving Eqs. (3) from which extract $\boldsymbol{\sigma}(\boldsymbol{u}_N^0(\boldsymbol{\lambda}^k))$ and $\boldsymbol{\sigma}(\boldsymbol{u}_D^0(\boldsymbol{\lambda}^k))$ on Γ_i.

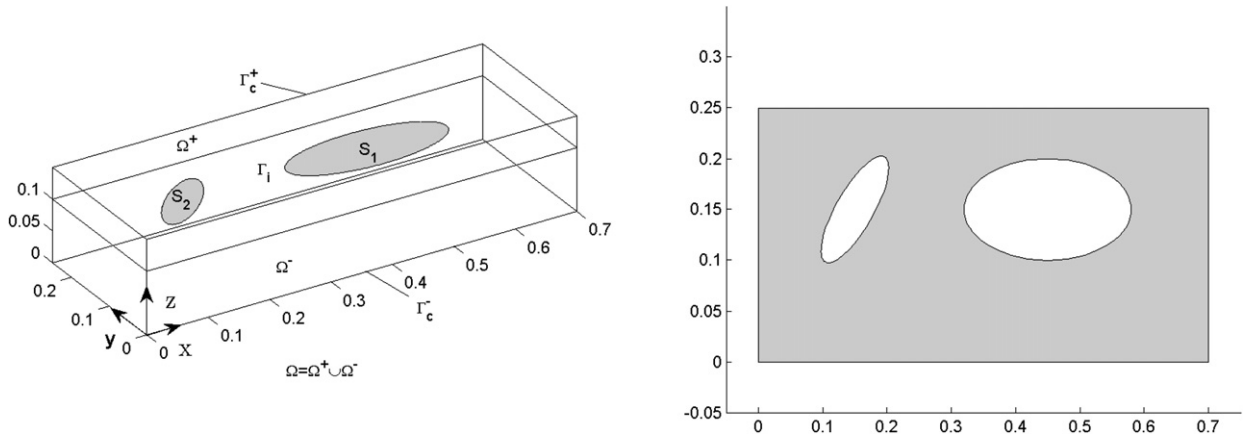

Fig. 1. Geometry of the cracked domain and the cracked interface Γ_i.

4. Numerical results

Our numerical experiment focuses on the detection of cracks on *a priori* known internal surface (coating defects or delamination in a composite material) inside a three-dimensional elastic body. Overdetermined elastostatic boundary data on a part of the outer surface are assumed to be known or can be measured. There is a great amount of literature on crack identification, though here we refer to papers [13] and [14] where they deal with overdetermined boundary data. The first deals with the elastostatic context while the second uses time-dependent measurements. The following example is inspired by the case studied in [13].

The cracked body consists of a cuboid with dimensions $70 \times 25 \times 15$ filled with homogeneous isotropic elastic material ($E = 200$ GPa, $\nu = 0.3$). It contains two elliptic cracks S_1 with main axes $a_1 = 13$ and $b_1 = 5$ parallel to the x and y directions, and S_2 with main axes $a_2 = 7$ and $b_2 = 2.5$ making an angle of 45° with x and y directions. The crack S_1 has its center at $(45, 15)$ and S_2 is centered at $(15, 15)$ on the planar internal surface $\Gamma_i = \{(x, y, z)^t \in \Omega / z = 10\}$ as shown in Fig. 1.

The boundary conditions are as follows: the left-hand side of the cuboid is clamped. The right-hand side is fixed in the y and z directions. The loading is a vertical constant traction field $\tilde{\boldsymbol{t}} = \pm(0, 0, 2)$ kPa applied respectively to the whole upper and lower surfaces. The remaining parts of the outer boundary are traction-free. The solid is discretized using linear tetrahedric three-dimensional finite elements with three degrees of freedom by node (8012 finite elements). $\Gamma_c = \Gamma_c^+ \cup \Gamma_c^-$ is discretized into 538 nodes whereas Γ_i is discretized into 999 nodes. The crack surfaces S_1 and S_2 are assumed to be traction-free, whereas on the remaining part of the internal plane $\Gamma_i \setminus (S_1 \cup S_2)$ the usual compatibility conditions are considered. The simulation is run using *synthetic data* generated by a finite element resolution of the direct problem. The software MATLAB is used to solve the direct and inverse problems. The numerical problems are solved by using GMRES algorithm with L-curve as stopping criteria. The L-curve is the plot in the logarithmic scale, for all iterations k, of the solution norm $\| \boldsymbol{\lambda}_k \|_2$ versus the corresponding residual norm $\| \boldsymbol{S}\boldsymbol{\lambda}_k - \boldsymbol{\chi} \|_2$ [15,16]. In [16] Hansen shows that for discrete ill-posed problems it turns out that the L-curve, always has a characteristic L-shaped appearance with a distinct corner separating the vertical and the horizontal parts of the curve and displays the trade-off between minimizing the residual norm and the solution norm (see Fig. 2 (right)).

In order to detect the cracks, two Cauchy problems are solved. The first P^+ is defined on the upper subdomain Ω^+ where the overspecified data are given only on the upper boundary Γ_c^+ and the unknowns are identified on the boundary Γ_i. The second Cauchy problem P^- is defined on the lower subdomain Ω^- where the overspecified data are given only on the lower boundary Γ_c^- and the unknowns are identified on the boundary Γ_i. Among the unknowns we are only interested with the displacements. If we denote by $\boldsymbol{u}^+$ (resp. $\boldsymbol{u}^-$) the displacements field on Γ_i provided by P^+ (resp. P^-), the cracks will be identified at the part of Γ_i where the discontinuity of the displacements vector $[\boldsymbol{u}^+ - \boldsymbol{u}^-]$ is still visible. To emphasize the reliability of the SP approach and to attest the stabilizing effect, a uniform white noise with null mean is applied to the Dirichlet data on Γ_c.

Fig. 2 (left) shows for a sample (P^+ with DSP) the error $e = \frac{\|(\boldsymbol{u}_{calc} - \boldsymbol{u}_{exact})\|_{L2(\Omega)}}{\|\boldsymbol{u}_{exact}\|_{L2(\Omega)}}$ as a function of the number of iterations k. It can be seen that the error e decreases rapidly over the first few iterations and then increases with respect to k: this property is called semi-convergence [1]. The iterative process has to be stopped at the point where the error e stops decreasing. Calvetti et al. [17] show that this point corresponds to the vertex of the L-curve (see Fig. 2 (right)).

Fig. 3 depicts the recovery of the discontinuity $[\boldsymbol{u}^+ - \boldsymbol{u}^-]$ across the interface Γ_i, using noise free data. It seems that the width of the crack has no influence on the accuracy of the reconstruction procedure: both cracks are well identified. However, the identification of the cracks by solving the primal Steklov–Poincaré equation is quite poor. We point out that the mesh described above is used for both approaches.

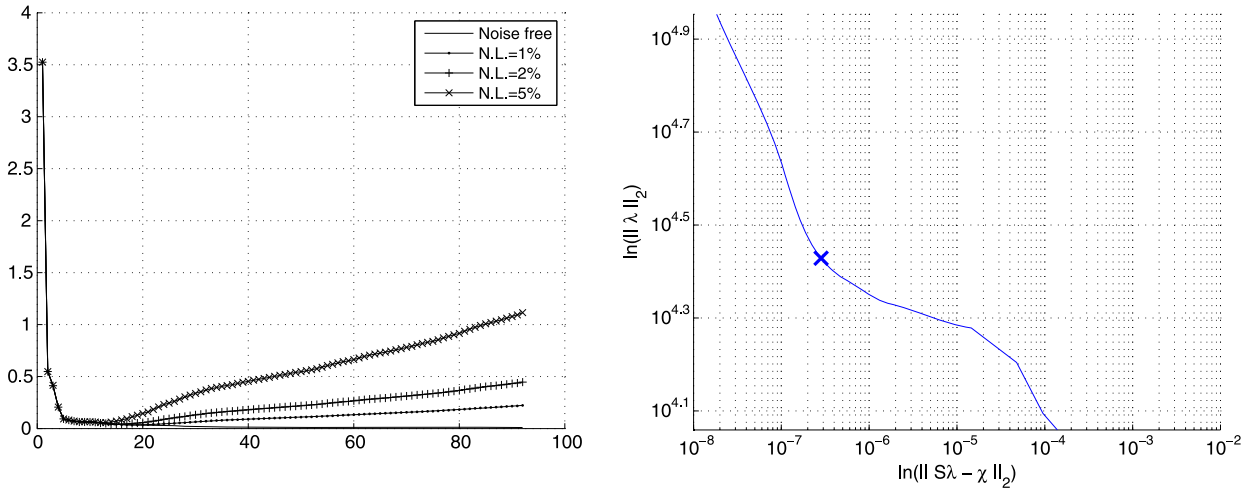

Fig. 2. Left: rate of convergence with different noise levels (N.L.). Right: L-curve (N.L. = 1%).

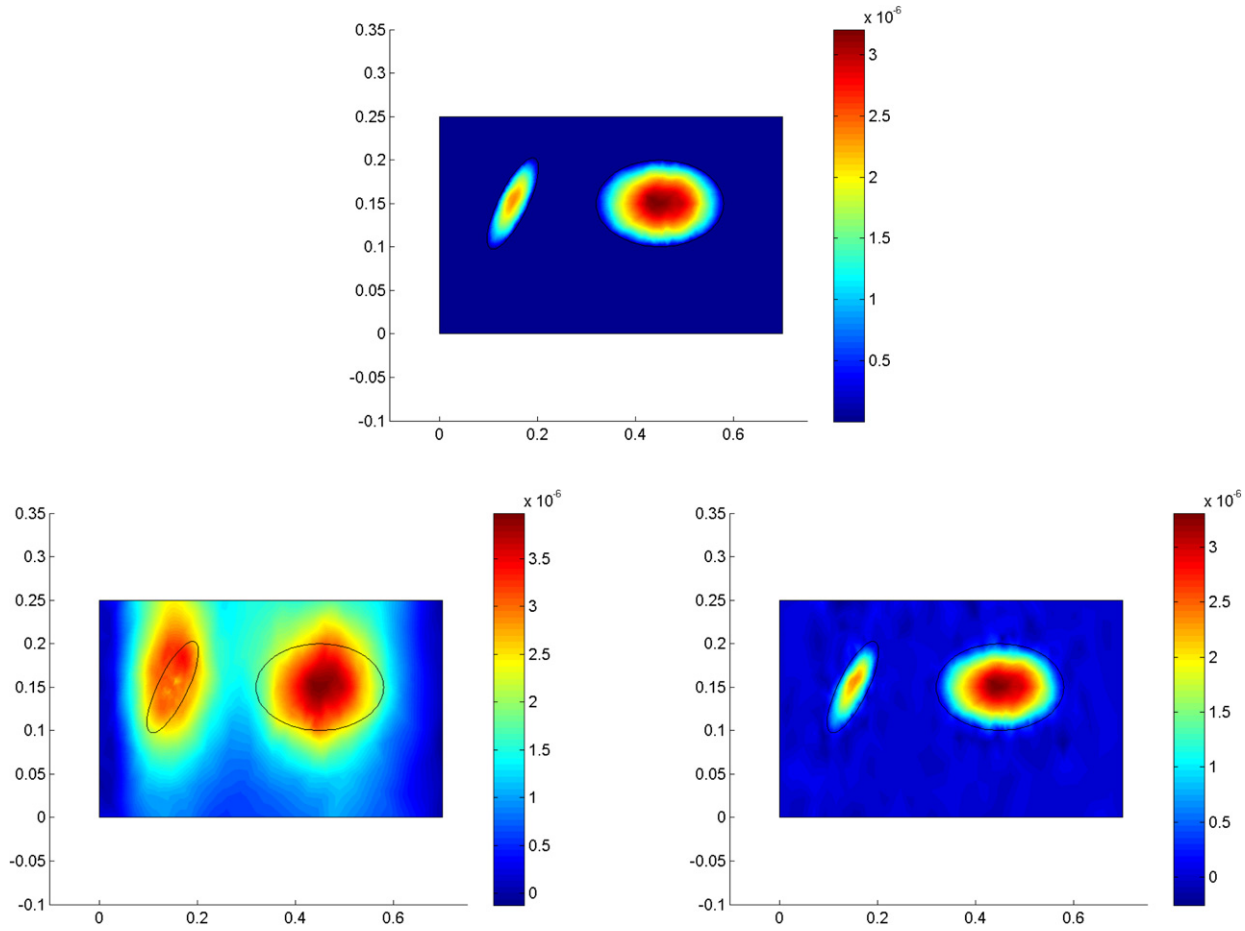

Fig. 3. Exact $[\boldsymbol{u}^+ - \boldsymbol{u}^-]$ through Γ_i (top), SP identification with noise-free data (bottom left), DSP identification with noise-free data (bottom right).

We consider now, for the inverse problem, a *synthetic data* obtained from the resolution of a direct problem with a different mesh (14 244 finite elements). $\Gamma_c = \Gamma_c^+ \cup \Gamma_c^-$ is discretized into 824 nodes whereas Γ_i is discretized into 1231 nodes. The inverse problem is solved by using the same mesh as the previous example. The data on Γ_c are then generated by linear interpolation of those given by the direct problem. Note that this approach comes to pollute the data with some noise. Fig. 4 shows that the DSP approach remains trustful for the identification while the SP one is deteriorating more and

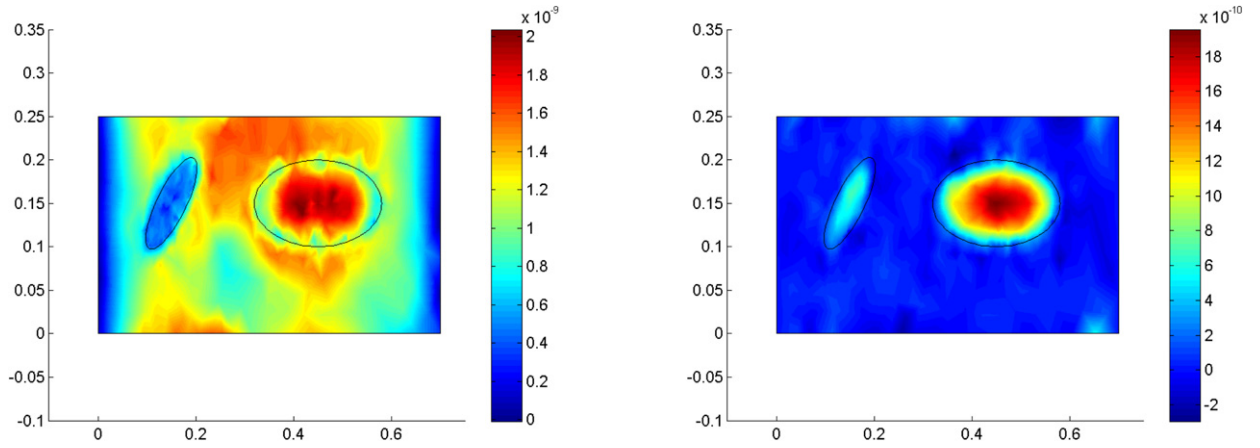

Fig. 4. Direct and inverse problems solved with different meshes. Left: SP identification (noise-free data). Right: DSP identification (noise-free data).

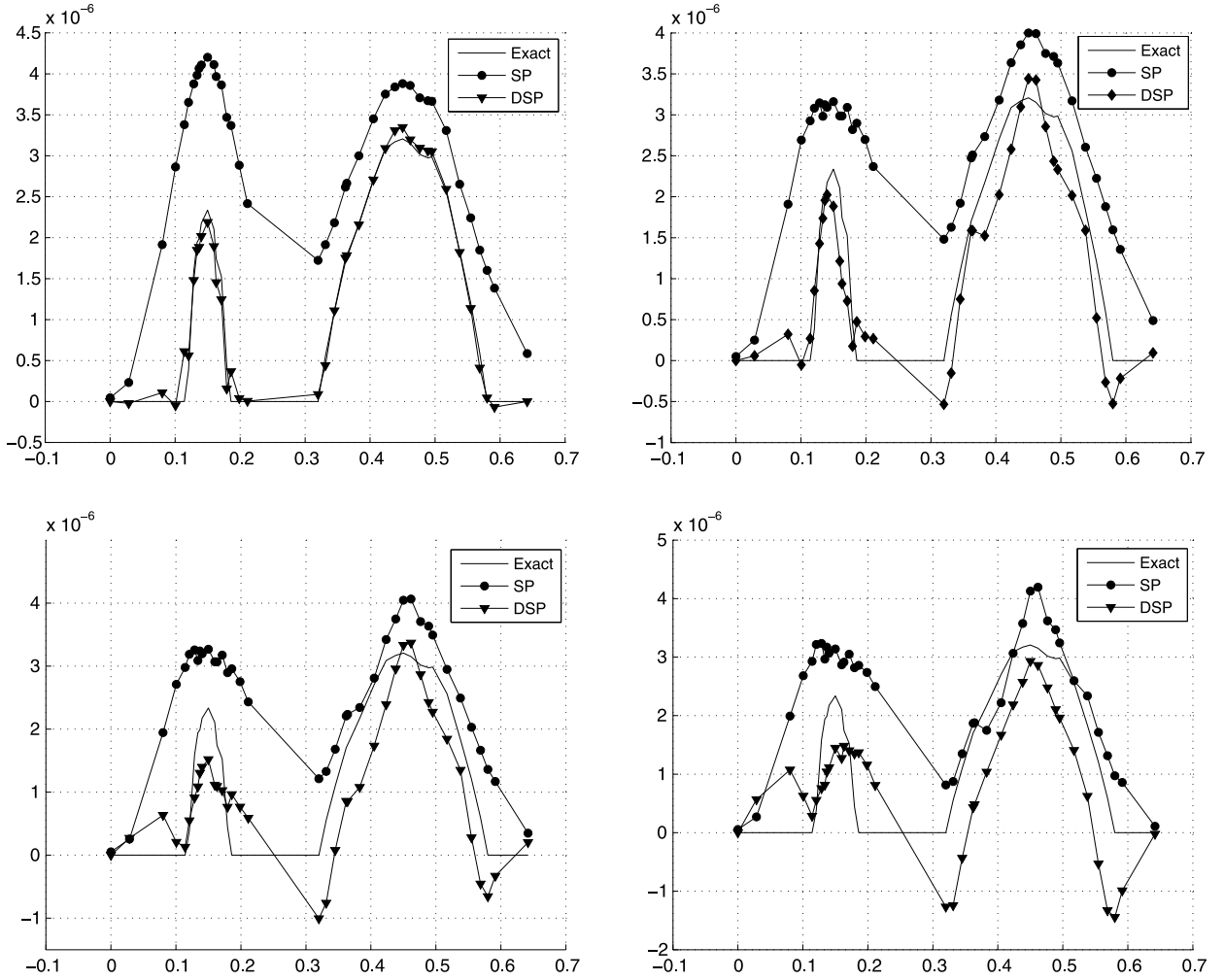

Fig. 5. Jump $[\boldsymbol{u}^+ - \boldsymbol{u}^-]$ through $\Gamma_i \cap (y = 0.15)$. Top left: noise-free data, top right: N.L. = 2%, bottom left: N.L. = 5%, bottom right: N.L. = 10%.

more. To highlight the superiority of the DSP approach, we depict in Fig. 5 the trace of the jump $[\boldsymbol{u}^+ - \boldsymbol{u}^-]$ on the vertical plan containing the centers of the cracks.

We observe that the DSP approach is more accurate than the SP one.

Table 1
Convergence speed and accuracy of KMF, SP and DSP algorithms for polluted Dirichlet data (noise level 2%).

Method	e^*_{P+}	k^*_{P+}	e^*_{P-}	k^*_{P-}
KMF	0.1820	31	0.1337	26
SP	0.0984	51	0.0590	28
DSP	0.0420	14	0.0314	22

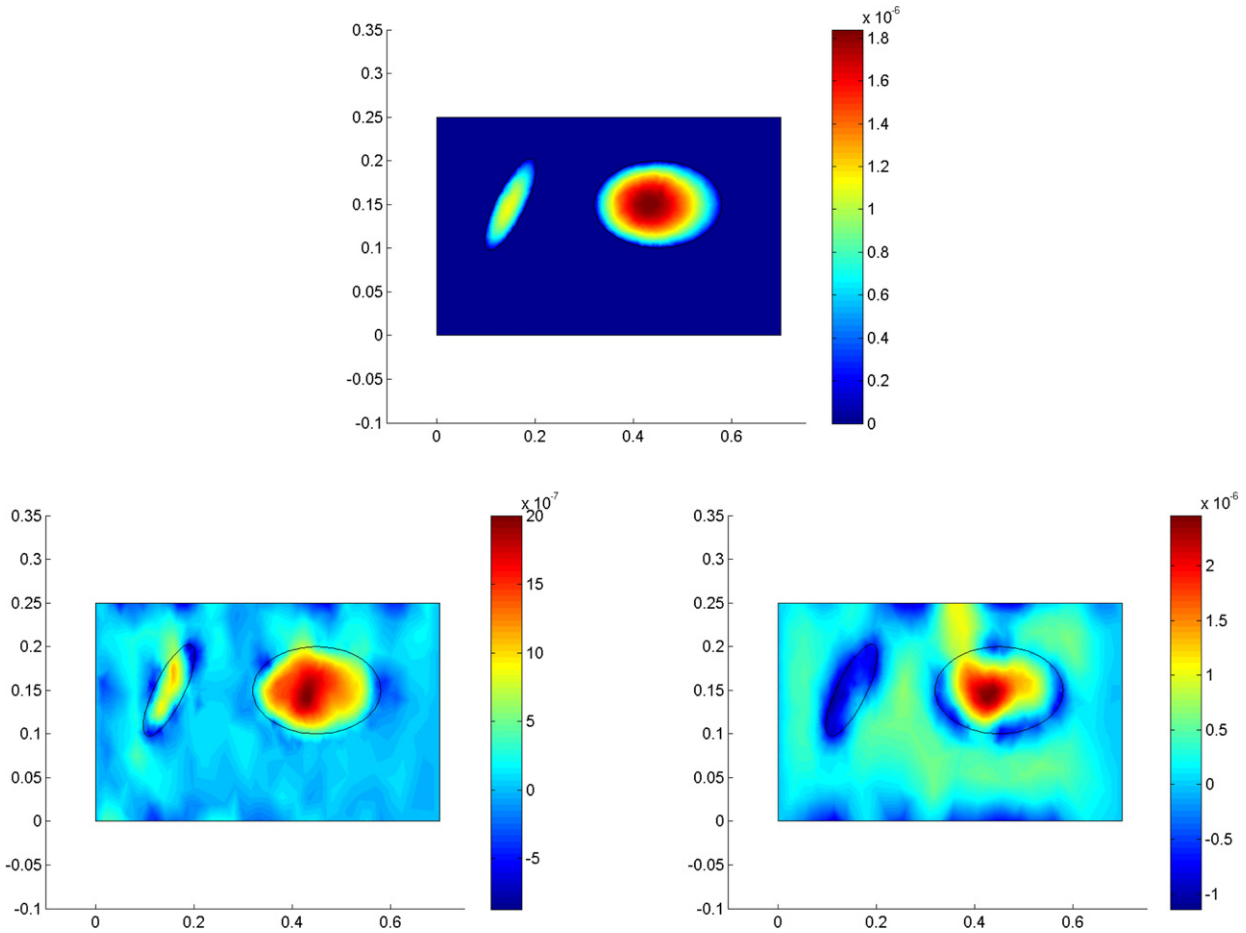

Fig. 6. Thick sample: Exact $[\boldsymbol{u}^+ - \boldsymbol{u}^-]$ through Γ_i (top), DSP identification (N.L. = 0%), DSP identification (N.L. = 1%)

Table 1 illustrates KMF, SP and DSP algorithms for noisy data. e^* and k^* denote respectively the relative L^2 error on the displacements on the hole domain Ω and the iteration number when the algorithm converges. We observe that the KMF algorithm has difficulties to converge. We can see also that the DSP algorithm clearly outperforms the KMF and SP ones.

Now we carry out a second experiment where the sample is more thick with deeper interface: the cracked body consists of a cuboid with dimensions $70 \times 25 \times 30$. The new planar internal surface is $\Gamma_i = \{(x, y, z)^t \in \Omega / z = 20\}$, all other characteristics of the sample and the cracks are not changed. The solid is discretized into 15 867 finite elements. $\Gamma_c = \Gamma_c^+ \cup \Gamma_c^-$ is discretized into 443 nodes whereas Γ_i is discretized into 1219 nodes.

The DSP approach is less accurate in the case of the thick sample but the cracks identification remains acceptable. For noisy data the reconstruction is not satisfactory (see Fig. 6).

5. Conclusion

In this work we presented two numerical methods for identifying cracks, lying in a *a priori* known plan, in a 3D elastic body: the primal and dual Steklov–Poincaré approaches. Both approaches were tested and compared each to other and to KMF one. For this application, the dual formulation is clearly more relevant than both of other approaches. Forthcoming work will include elastoplastic crack identification.

References

[1] J. Ben Abdallah, A conjugate gradient type method for the Steklov–Poincaré formulation of the Cauchy–Poisson problem, International Journal of Applied Mathematics and Mechanics 3 (2007) 27–40.
[2] J. Hadamard, Lectures on Cauchy's Problem in Linear Partial Differential Equation, Dover, New York, 1953.
[3] A. Quarteroni, A. Valli, Domain Decomposition Methods for Partial Differential Equations, Oxford University Press, Oxford, 1999.
[4] F. Ben Belgacem, H. El Fekih, On Cauchy's problem: I. A variational Steklov–Poincaré theory, Inverse Problem 21 (2005) 1915–1936.
[5] M. Azaiez, F. Ben Belgacem, H. El Fekih, On Cauchy's problem: II. Completion, regularization and approximation, Inverse Problems 22 (2006) 1307–1336.
[6] F. Ben Belgacem, Why is the Cauchy's problem severely ill-posed? Inverse Problems 23 (2008) 823–836.
[7] T.N. Baranger, S. Andrieux, Constitutive law gap functionals to solve Cauchy problem for a linear elliptic PDE: a review, http://hal.archives-ouvertes.fr/hal-00489572/fr/, 2010.
[8] V.A. Kozlov, V.G. Maz'ya, A.V. Fomin, An iterative method for solving the Cauchy problem for elliptic equations, Computational Mathematics and Mathematical Physics 31 (1991) 64–74.
[9] W.C. Yeih, T. Koya, T. Mura, An inverse problem in elasticity with partially overspecified boundary conditions. I. Theoretical approach, Transactions of the ASME Journal of Applied Mechanics 60 (1993) 595–600.
[10] S. Andrieux, T.N. Baranger, An energy error-based method for the resolution of the Cauchy problem in 3D linear elasticity, Computer Methods in Applied Mechanics and Engineering 197 (2008) 902–920.
[11] T.N. Baranger, S. Andrieux, Data completion for linear symmetric operators as a Cauchy problem: an efficient method via energy like error minimization, Vietnam Journal of Mechanics, VAST 31 (2009) 247–261.
[12] T.N. Baranger, S. Andrieux, An optimization approach to solve Cauchy problem in linear elasticity, Journal of Structural and Multidisciplinary Optimization 35 (2008) 141–152.
[13] W. Weikl, H. Andrä, E. Schnack, An alternating iterative algorithm for the reconstruction of internal cracks in a three-dimensional solid body, Inverse Problems 17 (2001) 1957–1975.
[14] C. Bellis, M. Bonnet, Crack identification by 3D time-domain elastic or acoustic topological sensitivity, C. R. Mecanique 337 (2009) 124–130.
[15] M. Hanke, Conjugate Gradient Type Methods for Ill-Posed Problems, Pitman Research Notes in Mathematics, vol. 327, CRC Press, United States, 1995.
[16] P.C. Hansen, Rank-Deficient and Discrete Ill-Posed Problems, SIAM, Philadelphia, 1998.
[17] D. Calvetti, B. Lewis, L. Reichel, GMRES, L-curves, and discrete ill-posed problems, BIT 42 (2002) 44–65.